

Immunohistochemical analysis-based proteomic subclassification of newly diagnosed glioblastomas

Kazuya Motomura,¹ Atsushi Natsume,^{1,11} Reiko Watanabe,² Ichiro Ito,² Yukinari Kato,³ Hiroyuki Momota,¹ Ryo Nishikawa,⁴ Kazuhiko Mishima,⁴ Yoko Nakasu,⁵ Tatsuya Abe,⁶ Hiroki Namba,⁷ Yoichi Nakazato,⁸ Hiroshi Tashiro,² Ichiro Takeuchi,⁹ Tsutomu Mori¹⁰ and Toshihiko Wakabayashi¹

¹Department of Neurosurgery, Nagoya University School of Medicine, Nagoya; ²Division of Diagnostic Pathology, Shizuoka Cancer Center, Shizuoka; ³Molecular Tumor Marker Research Team, Faculty of Medicine, The Oncology Research Center, Advanced Molecular Epidemiology Research Institute, Yamagata University, Yamagata; ⁴Department of Neurosurgery, Saitama Medical University International Center, Saitama; ⁵Department of Neurosurgery, Shizuoka Cancer Center, Shizuoka; ⁶Department of Neurosurgery, Oita University School of Medicine, Oita; ⁷Department of Neurosurgery, Hamamatsu University School of Medicine, Hamamatsu; ⁸Department of Human Pathology, Gunma University School of Medicine, Gunma; ⁹Department of Engineering, Nagoya Institute of Technology, Nagoya; ¹⁰Department of Human Lifesciences, Fukushima Medical University School of Nursing, Fukushima, Japan

(Received February 16, 2012/Revised June 20, 2012/Accepted June 21, 2012/Accepted manuscript online July 2, 2012)

Recent gene expression and copy number profilings of glioblastoma multiforme (GBM) by The Cancer Genome Atlas (TCGA) Research Network suggest the existence of distinct subtypes of this tumor. However, these approaches might not be easily applicable in routine clinical practice. In the current study, we aimed to establish a proteomics-based subclassification of GBM by integrating their genomic and epigenomic profiles. We subclassified 79 newly diagnosed GBM based on expression patterns determined by comprehensive immunohistochemical observation in combination with their DNA copy number and DNA methylation patterns. The clinical relevance of our classification was independently validated in TCGA datasets. Consensus clustering identified the four distinct GBM subtypes: Oligodendrocyte Precursor (OPC) type, Differentiated Oligodendrocyte (DOC) type, Astrocytic Mesenchymal (AsMes) type and Mixed type. The OPC type was characterized by highly positive scores of *Olig2*, *PDGFRA*, *p16*, *p53* and synaptophysin. In contrast, the AsMes type was strongly associated with strong expressions of nestin, CD44 and podoplanin, with a high glial fibrillary acidic protein score. The median overall survival of OPC-type patients was significantly longer than that of the AsMes-type patients (19.9 vs 12.8 months). This finding was in agreement with the OncoPrint analysis of TCGA datasets, which revealed that *PDGFRA* and *Olig2* were favorable prognostic factors and podoplanin and CD44 were associated with a poor clinical outcome. This is the first study to establish a subclassification of GBM on the basis of immunohistochemical analysis. Our study will shed light on personalized therapies that might be feasible in daily neuropathological practice. (*Cancer Sci*, doi: 10.1111/j.1349-7006.2012.02377.x, 2012)

Glioblastoma multiforme (GBM) is one of the most common and highly malignant brain tumors in the primary central nervous system in adults. GBM was one of the first tumor types registered in The Cancer Genome Atlas (TCGA), which is a project that catalogs genomic abnormalities involved in the development of cancer.^(1,2) The techniques currently used in TCGA study for the detection of abnormalities include gene expression profiling, copy number variation profiling, single-nucleotide polymorphism genotyping, genome-wide methylation profiling,⁽³⁾ microRNA profiling⁽⁴⁾ and exon sequencing. Since the publication of the first TCGA Network paper,⁽¹⁾ several groups within the TCGA network have presented the results of highly detailed analyses of GBM. Verhaak *et al.*⁽⁵⁾ recently subclassified GBM into Proneural, Neural, Classical and Mesenchymal subtypes by integrating multidimensional data on gene expression, somatic mutations and

DNA copy number. The main features of the Proneural class are focal amplification of *PDGFRA*, *IDH1* mutation, and *TP53* mutation and/or loss of heterozygosity. Moreover, high expression of genes associated with oligodendrocyte development, such as *PDGFRA*, *NKX2-2* and *OLIG2*, were also associated with this subtype. The Neural subtype is characterized by the expression of neuron markers, such as *NEFL*, *GABRA1*, *SYTI* and *SLC12A5*. The Classical subtype features high *EGFR* expression associated with chromosome 7 amplification and low expression of *p16INK4A* and *p14ARF*, resulting from a focal 9p21.3 homozygous deletion. Neural stem cell markers, such as nestin, as well as components of the Notch and Sonic hedgehog signaling pathways, are highly expressed in the Classical type. The Mesenchymal subtype is characterized by focal hemizygous deletions at 17q11.2 that contains *NF1* and high expression of *YKL-40* (*CHI3LI*), *MET*, *CD44* and *MERTK*. This classification of GBM using gene expression profiles (TCGA) may address the important issue of the inability to define different patient outcomes on the basis of histopathological features. For ultimately establishing a simple classification of groups of patients with GBM according to clinicopathological factors, a protein-based immunohistochemical approach, which is routinely used in most neuropathology laboratories, needs to be applied to avoid more complex molecular biology techniques.⁽⁶⁾

In the present study, we analyzed 79 archival GBM samples by immunohistochemistry using antibodies against 16 proteins selected based on Verhaak's classification for immunohistochemical analysis-based GBM subclassification, including Proneural (*Olig2*, *IDH1-R132H*,⁽⁷⁾ *p53*, *PDGFRA* and *PDGFB*), Neural (synaptophysin), Classical (*p16*, *EGFR*, *Hes-1* and nestin) and Mesenchymal types (*VEGF*, *YKL-40*, *CD44* and podoplanin [*PDPN*]), as well as high glial fibrillary acidic protein (GFAP) and Ki-67, and incorporated the results into the existing genomic and epigenomic data for these samples. We successfully identified clinically relevant subtypes that partially overlap the Verhaak subgroups.

Materials and Methods

Tumor samples. Samples from 79 consecutive patients with newly diagnosed GBM from several academic tertiary-care neurosurgical institutions were collected. All the samples were collected from GBM patients treated with temozolomide

¹¹To whom correspondence should be addressed.
E-mail: anatsume@med.nagoya-u.ac.jp

(TMZ). Paraffin-embedded surgical samples were collected for immunohistochemical analysis. All of the specimens had been fixed in 10% formalin. Three neuropathologists (Y.N., R.W. and I.I.) independently confirmed the GBM diagnosis according to WHO guidelines.^(8,9)

Matched fresh-frozen tissue samples were also obtained. DNA was prepared as described previously.⁽¹⁰⁾ All the patients provided their written informed consent for molecular studies of their tumor at each participating hospital. The study had the approval of each of the ethics committees of the Nagoya University Hospital, Shizuoka Cancer Center, Saitama Medical University Hospital, Oita University Hospital and Hamamatsu Medical University Hospital (title, "Genetic analysis associated with brain tumor"). This study complied with all the provisions of the Declaration of Helsinki.

Immunohistochemical analysis. Immunohistochemical analysis was performed as previously described.⁽¹¹⁾ The antibodies used in the present study are summarized in Table S1. For each immunostained slide, the percentage of positively stained GBM cells on a given slide was evaluated and scored, as shown in Table S2. This procedure was performed by two pathologists (R.W. and I.I.), and scores were decided through a consensus. This process was performed twice, and the final scores were determined at the second round before clustering analysis.

Multiplex ligation-dependent probe amplification. Multiplex ligation-dependent probe amplification (MLPA) was used for determining allelic losses and gains of the gene in the tumor samples. The analysis was performed using the SALSA MLPA kit P088-B1 and P105-C1 in accordance with the manufacturer's protocol (MRC Holland, Amsterdam, the Netherlands).^(12–15) All the procedures were performed as described previously.⁽¹⁰⁾

Pyrosequencing. Tumor DNA was modified with bisulfate by using the EpiTect bisulfite kit (Qiagen, Courtaboeuf Cedex, France). Pyrosequencing technology was used to determine the methylation status of the CpG island region of MGMT, as described previously.^(10,16,17)

TP53 and IDH1/IDH2 sequencing. Direct sequencing of *TP53* exons 5–8, which contain mutation hot spots in gliomas, and *IDH1/2* was performed as previously described.^(10,18–20) For *IDH* sequencing, 129 and 150-bp fragments spanning the sequences encoding the catalytic domains of *IDH1* (including codon 132) and *IDH2* (including codon 172), respectively, were amplified.

Oncomine data analysis. An independent set of 401 GBM mRNA expression profiles was analyzed by using the Oncomine Premium Research Edition to assess subtype reproducibility. Details of the standardized normalization techniques and statistical calculations can be found on the Oncomine website (<https://www.oncomine.com>).

Statistical analysis. To identify distinct GBM subclasses, we applied consensus clustering to our immunohistochemical data.⁽²¹⁾ Consensus clustering has been used in many recent biomedical studies because it can estimate the statistical stability of the identified clusters.⁽⁵⁾ Within the consensus clustering, *K*-means clustering with the Euclidean distance metric was used as the basic clustering option. For *K* ranging from 2 to 5, the *K*-means clustering was run over 10 000 iterations with a subsampling ratio of 0.8 for estimating the consensus matrix. For the purpose of visualization and cluster identification, hierarchical clustering with the Euclidean distance metric and the complete linkage option was applied to the estimated consensus matrix. The identified clusters were validated and confirmed using consensus cluster dependence factor plot analysis⁽²¹⁾ and silhouette analysis.⁽²²⁾ To visualize the four identified clusters, principal component analysis (PCA) was applied to the immunohistochemical data and 3-D ellipsoids representing the covariance structure of each cluster were

drawn in the 3-D plots of the first three principal components. Most of the statistical analyses (except the 3-D plot, which was generated by JMP ver.9.0) were performed using *R*.⁽²³⁾ We used a Kruskal–Wallis rank test to analyze the differences between the four GBM subgroups, and the pairwise differences in the expressions of 16 proteins and genetic/epigenetic alterations between each subgroup and the other three subgroups. The differences between the GBM subtypes with $P < 0.005$ were considered to be statistically significant in a more stringent manner, as the four clusters themselves are determined by the expression of these proteins and genetic/epigenetic alterations. Statistical analysis of survival was performed using the statistical software *SPSS* version 17.0 for Windows (*SPSS*, Chicago, IL, USA). Survival was estimated using the Kaplan–Meier method and survival curves were compared using the log-rank test.

Results

Patient characteristics. The summary of the GBM patient and treatment characteristics is shown in Table S3. All 79 patients received surgical treatment followed by standard TMZ-based chemotherapy and conventional radiation therapy, with daily concurrent TMZ at 75 mg/m² throughout the course of the radiation therapy.⁽²⁴⁾

This study population included 50 male and 29 female patients aged 13–84 years (median age, 61 years). The median preoperative Eastern Cooperative Oncology Group performance status (ECOG PS) score at diagnosis was one (range, 0–4); the preoperative ECOG PS score was <1 in the case of 48 patients (60.8%). All the tumors were located in the supratentorial region: 60 tumors (75.9%) were located in the superficial area (cortical or subcortical area), and 19 (24.1%) were located in deep anatomical structures such as the basal ganglia and corpus callosum. Surgical gross total resection (GTR) was achieved in 24 patients (30.4%), and non-GTR was performed in 55 patients (69.6%).

Consensus clustering subclassifies four subtypes. The GBM subtypes identified by consensus clustering are shown in Figure 1, with clustering stability increasing from $K = 2$ to $K = 4$, but not to $K = 5$ (Figs 1,2). Furthermore, the identified clusters were confirmed on the basis of their positive silhouette width,⁽²²⁾ indicating higher similarity to their own class than to a member of any other class (Fig. 3).

According to the results, the 79 GBM cases examined were basically classified into four clusters: clusters I (nine cases), II (17 cases), III (14 cases) and IV (39 cases), depending on the branch length, which represents the correlation between the scoring data and the similarity in GBM tumor samples (Fig. 4). This analysis identified four discrete groups of sample sets that differed markedly in GBM protein expression. The 3-D ellipsoid of each cluster in PCA in Figure 5 also suggests the clear separations of each cluster. All the scores for the immunohistochemical analysis and genetic/epigenetic data lists for all the analyses are available in Table S4.

These protein groups were named according to the distribution and biological function of the representative protein expressions of Olig2, IDH1-R132H, PDGFRA, p16, EGFR, Hes-1, nestin, CD44, PDPN and GFAP; that is, Oligodendrocyte Precursor (OPC) type, Differentiated Oligodendrocyte (DOC) type, Astrocytic Mesenchymal (AsMes) type, and Mixed type. Figure 6 shows the immunohistochemical staining pattern in the 79 GBM cases, aligned according to the four identified clusters, indicating similarity in immunohistochemical staining patterns within each cluster.

Differentiated Oligodendrocyte type. All the samples clustered in this type showed high positivity for the oligodendroglial marker Olig2 and small round cell morphology (Table 1,

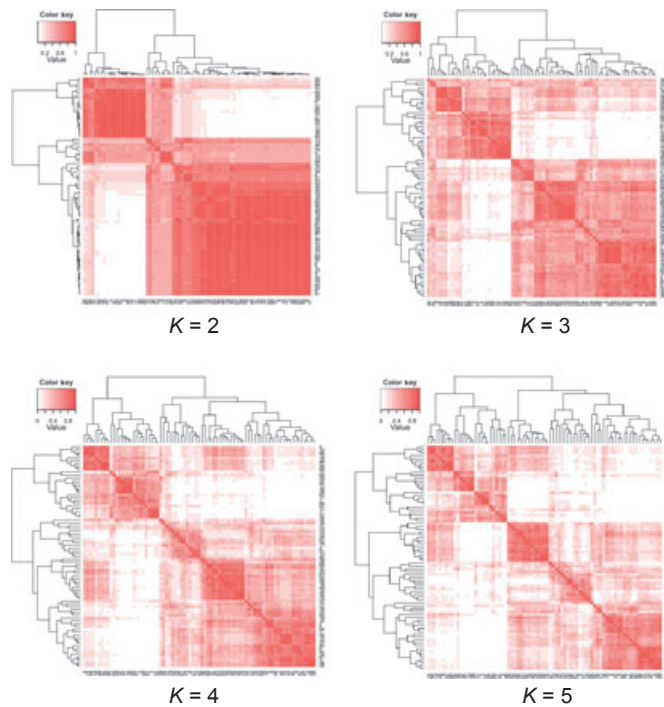


Fig. 1. Consensus matrix heat maps demonstrating the presence of several clusters within the 79 samples of GBM for $K = 2$ to $K = 5$ cluster assignments for each cluster method. The red areas identify the similarity between the samples and display samples clustered together across the bootstrap analysis.

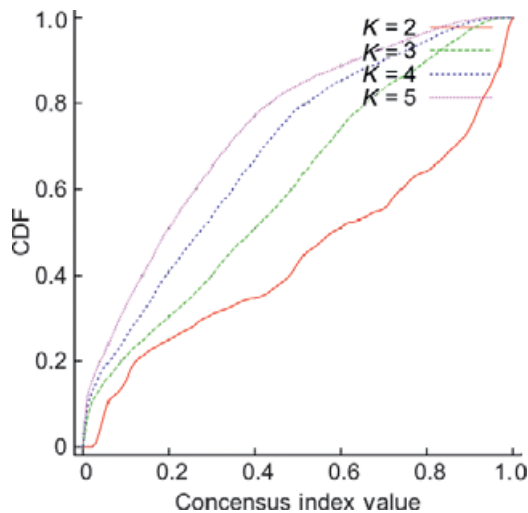


Fig. 2. Consensus clustering cluster dependence factor (CDF) for $K = 2$ to $K = 5$.

Fig. 6). Furthermore, negativity for p53 and p16 was noted. GFAP was almost always negative in the tumor cell cytoplasm (Fig. 6). Genetically, 1p/19q co-deletion and *CDKN2A* loss were more frequently observed in this cluster than in the other clusters (Fig. 7). The presence of 1p/19q co-deletion was assessed if the DNA copy numbers at a minimum of three adjacent loci were less than 0.65 at 1p and 19q.

Oligodendrocyte Precursor type. This cluster was characterized by highly positive scores for PDGFRA, p16, and p53 in addition to a highly positive score for an oligodendroglial marker, Olig2 (Fig. 6). From the perspective that oligodendrocytes arise during development from oligodendrocyte precursors,

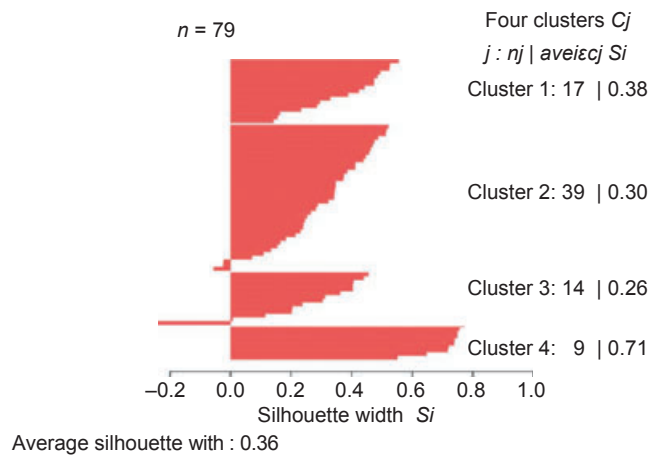


Fig. 3. Silhouette plot for identification of core samples.

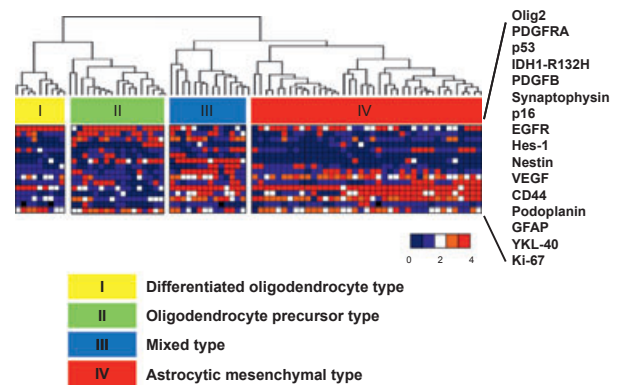


Fig. 4. Immunohistochemical analysis-based subgroups and comparison with genetic and epigenetic alterations. The heat map and dendrogram show the expression profiles of 16 proteins well characterized in glioblastoma multiforme (GBM) and demonstrate the significant pattern of differential expression among the four subgroups. The statistical significance of the differential protein expression was determined using one-way ANOVA.

which can be identified by the expression of a number of antigens, including PDGFRA, this subgroup was named the Oligodendrocyte Precursor (OPC) type. On the contrary, few samples had high scores for nestin, CD44, and PDPN in this group (Table 1; Fig. 6). It is interesting that the genetic alterations were observed in *IDH1* mutations (23.5%) and *TP53* mutations (52.9%). These findings were consistent with the results of protein expression. Methylation of the *MGMT* promoter (41.2%) was most frequently detected in this cluster (Fig. 7).

Astrocytic Mesenchymal type. This type was generally characterized by: strong membranous and/or stromal positivity for CD44 and/or PDPN; cytoplasmic positivity for GFAP and/or nestin in tumor cells; total negativity for p16, except in the case of four patients; and sparse positivity for p53 (Table 1, Fig. 6). Morphologically, the tumor cells observed in the H&E-stained sections showed pleomorphism. In striking contrast to the OPC type, this type was also strongly associated with low levels of Olig2, IDH1-R132H, p53, p16 and PDGFRA, and rather strong GFAP expression (Table 1). These findings suggest that this cluster was strongly characterized by astrocytic features.

Genetically, *IDH1* and *TP53* mutations were rare in this group. Furthermore, methylation of the *MGMT* promoter (20.5%) was detected at a low frequency (Fig. 7).

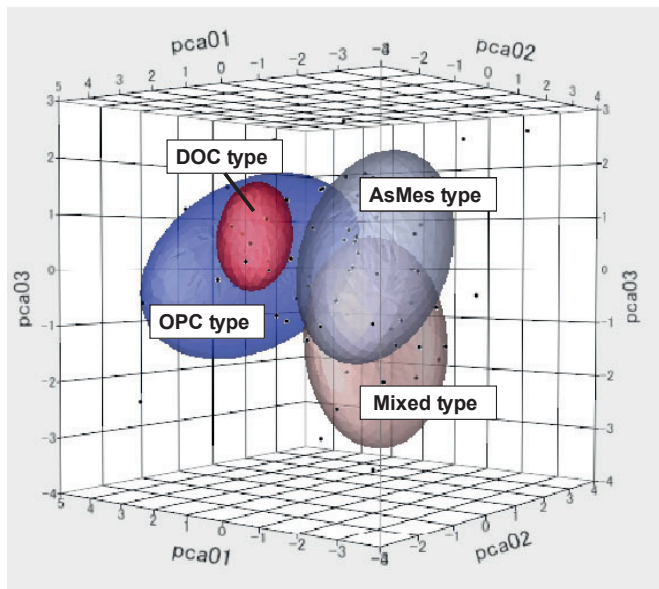


Fig. 5. Principal component analysis (PCA) of four glioblastoma multiforme (GBM) subtypes. Ellipsoid bodies represent two SD of the data distribution for each subgroup.

Mixed type. Compared with TCGA's Classical-type markers, frequent expressions of p16 (79%), EGFR (36%) and Hes-1 (64%), as well as a Proneural-type marker, p53 (64%), were predominant in this class (Table 1, Fig. 6).

Strong expression of the downstream Notch transcriptional target Hes-1 suggested that the prominent Notch-Hes-1 pathway was activated in this class. Furthermore, this cluster was characterized by positivity for CD44 and GFAP, and morphologically, by tumor cells with eosinophilic cytoplasm. This morphological characteristic was compatible with limited or scant positivity for Olig2. CD44 and PDPN were detected in many tumor cells.

In addition, this cluster had a genetically high frequency of *EGFR* amplification (57.1%) and low frequency of *CDKN2A* loss, and these findings are consistent with the protein expression data (Fig. 7). Thus, we named this cluster Mixed type because it shares characteristics of the OPC type and AsMes type or those of TCGA's Proneural and Classical types.

Morphological characteristics of the four types. On the H&E-stained sections, the morphological findings of the four types were fairly characteristic, although not specific (Fig. 8). In the DOC type, the tumor cells had small round or oval nuclei, scant cytoplasm and few cytoplasmic processes. The tumor cell nuclei showed a fine and diffuse chromatin (Fig. 8a,b). In some cases in which the tumor cells had faint processes, the cells tended to gather around vessels.

In the OPC type, in addition to small round or oval nucleated cells similar to those of the DOC type, there were scattered intermediate to large pleomorphic and/or multinucleated neoplastic cells, cells with vesicular chromatin, and/or cells with short spindle-shaped or irregularly-shaped nuclei that were slightly larger than the small round or oval cells (Fig. 8c,d).

In the AsMes type, many neoplastic cells had spindle-shaped nuclei and almost bipolar, distinct cytoplasmic processes. They were generally arranged in bundle-like and interlacing patterns. Some neoplastic cells had nuclei with vesicular open chromatin. The boundaries of the cytoplasmic processes were generally well defined (Fig. 8e,f).

In the Mixed type, there were scattered large pleomorphic cells on a background of intermediate or small cells. The latter background cells had irregularly-shaped nuclei and spindle-

shaped cytoplasmic processes that were haphazardly arranged, in comparison with the bundle formations in the AsMes type (Fig. 8g,h).

Overview of the immunohistochemical data and genomic/epigenomic profiles across the four glioblastoma multiforme subtypes. We sought to select the most significant factors to distinguish the four GBM subgroups by a Kruskal–Wallis rank test. As indicated in Tables S5 and S6, the differences between the GBM subtypes showing $P < 0.005$ were considered to be statistically significant in a more stringent manner, as the four clusters themselves are determined by the expression of these proteins and genetic/epigenetic alterations. Of these, Olig2, p53, PDGFRA, synaptophysin, p16 and the *IDH1* mutation were positively correlated with the OPC type, whereas positive correlations with nestin, PDPN, CD44 and GFAP were predominant in the AsMes type. The DOC type showed a significant positive correlation with the p16 expression in the Mixed type.

Proteomic clusters correlate with survival. The Kaplan–Meier survival analysis revealed that the four proteomic clusters differed significantly in their correlation with survival (Fig. 9 and Table 2). There were no significant differences in any of the clinical parameters (i.e. age, sex, preoperative ECOG PS, tumor location and extent of resection; Table S3) between the four cluster groups, as determined using the Fisher exact test.

It is interesting that the median overall survival (OS) associated with the OPC type was significantly longer (19.9 months [95% CI, 8.3–31.4]) than that of the patients with the AsMes type (12.8 months [95% CI, 10.0–15.7; $P = 0.041$]; Fig. 9). The difference was statistically significant, as determined by the log-rank test and univariate analysis. These findings were consistent with the OPC type being characterized by higher positive scores for IDH1-R132H (29%) in the immunohistochemical analysis and a high frequency of *IDH1* mutation (23.5%) in the genetic analysis, which are known to predict long-term survival.⁽²⁵⁾ Although the survival period of the patients in the Mixed type appeared to be the longest (median OS: 21.3 months [95% CI, 7.9–34.8]) among those of the other subgroups, the difference between these three subgroups was not statistically significant, presumably owing to the limited sample size in this study; the Kaplan–Meier curve of the DOC type (median OS: 14.8 months [95% CI, 2.6–27.0]) was similar to those of the OPC and Mixed types (Fig. 9).

Subgroup-specific outcome based on mRNA expression in The Cancer Genome Atlas datasets. An independent set of 401 GBM mRNA expression profiles was compiled from the Oncomine Premium Research Edition to assess subtype reproducibility. Among our selected 16 protein markers, information about the mRNA expressions of 12 markers and clinical outcomes could be obtained from TCGA brain dataset. IDH1-R132H, p53, p16 and Ki-67 were not available in the 401 GBM mRNA expression profiles of TCGA dataset because IDH1-R132H and p53 antibodies were used to detect mutation status, and this did not correlate with the mRNA expression of each gene. Moreover, because p16 protein expression correlates with the homozygous deletion of *CDKN2A*, we also excluded this protein from the analysis. In this analysis, the Olig2, PDGFRA and PDGFRA mRNA expression levels were significantly low in the tumors of patients who died at 1 year compared with those who survived for 1 year after the treatment. Notably, PDGFRA was the most favorable prognostic factor among these factors ($P = 0.002$; Fig. 10 and Tables 3 and 4).

Furthermore, PDPN, CD44, YKL-40 and EGFR mRNA were significantly overexpressed in the tumors of the patients who died 1 year after the treatment. These results indicate that PDPN is significantly associated with a poor clinical outcome ($P = 0.0003$; Fig. 10).

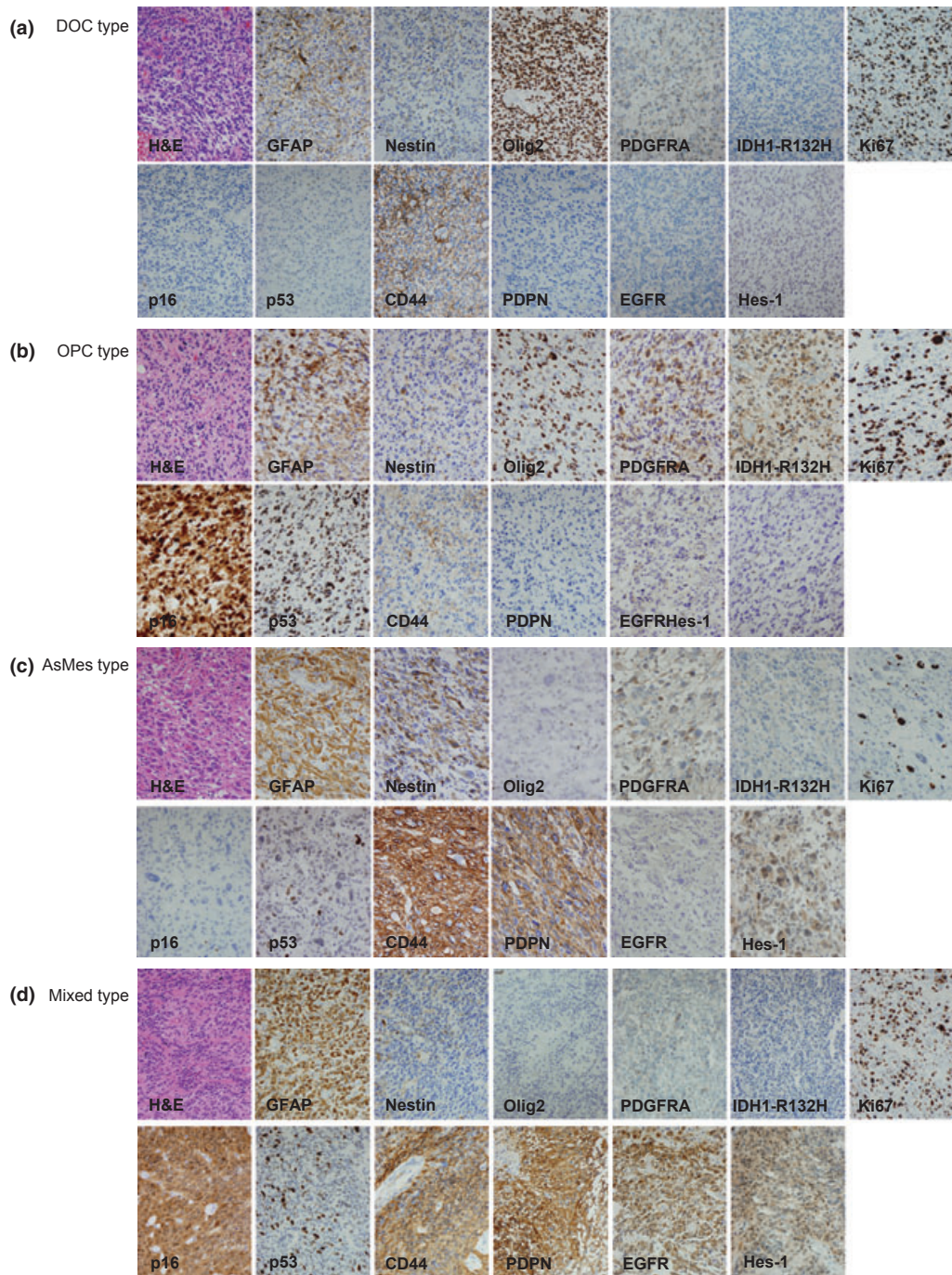


Fig. 6. Representative immunohistochemical images used in this study. (a) Differentiated Oligodendrocyte type (DOC type), glioblastoma multi-forme (GBM) case.44. (b) Oligodendrocyte Precursor type (OPC type), GBM case.01. (c) Astrocytic Mesenchymal type (AsMes type), GBM case 03. (d) Mixed type, GBM case 04.

Discussion

A large number of studies have shown that GBM can be classified by gene and protein expression profiling.^(5,26–28) The TCGA Research Network classifies GBM according to gene expression profiles into Proneural, Neural, Classical and Mesenchymal subtypes.⁽⁵⁾ However, these transcriptomic approaches might not be easily applied in routine clinical practice because complicated techniques are necessary to perform several of the experiments. Compared with these approaches, an immunohistochemistry-based approach could have widespread utility in the clinical set-

ting and lead to significantly improved patient stratification. The goal of the current study was to subclassify GBM using an immunohistochemical approach that is feasible in daily neuropathological practice, using a dataset from the TCGA Research Network as a reference. Our classification based on immunohistochemical analyses may enable the prediction of clinical chemosensitivity and survival in TMZ-treated patients with GBM.

Identification of four novel clusters by immunohistochemical analysis. We identified four novel clusters (OPC type, DOC type, AsMes type and Mixed type) with a considerably different expression profile of GBM tumors; to our knowledge, such an

Table 1. Frequency of positive score ≥ 3

Proteins	DOC	OPC	Mixed	AsMes	Total
	type (n = 9) (%)	type (n = 17) (%)	type (n = 14) (%)	type (n = 39) (%)	
Proneural					
Olig2	9 (100)	14 (82)	4 (29)	16 (41)	43
IDH1-R132H	0 (0)	5 (29)	0 (0)	1 (3)	6
p53	1 (11)	9 (53)	9 (64)	5 (13)	24
PDGFRA	3 (33)	10 (59)	5 (36)	3 (8)	21
PDGFB	2 (22)	1 (6)	5 (35)	9 (23)	17
Neural					
Synaptophysin	0 (0)	3 (18)	3 (21)	0 (0)	6
Classical					
p16	0 (0)	9 (53)	11 (79)	2 (5)	22
EGFR	0 (0)	0 (0)	5 (36)	5 (13)	10
Hes-1	0 (0)	3 (17)	9 (64)	11 (28)	23
Nestin	2 (22)	2 (12)	4 (29)	24 (62)	32
Mesenchymal					
VEGF	1 (11)	6 (35)	4 (29)	11 (28)	22
YKL-40	0 (0)	1 (6)	0 (0)	2 (5)	3
Podoplanin	0 (0)	0 (0)	4 (29)	18 (46)	22
CD44	5 (56)	1 (6)	11 (79)	37 (95)	54
GFAP	0 (0)	3 (18)	10 (71)	32 (82)	45
Ki-67	5 (56)	11 (65)	5 (29)	18 (46)	39

AsMes, astrocytic mesenchymal; DOC, differentiated oligodendrocyte; OPC, oligodendrocyte precursor.

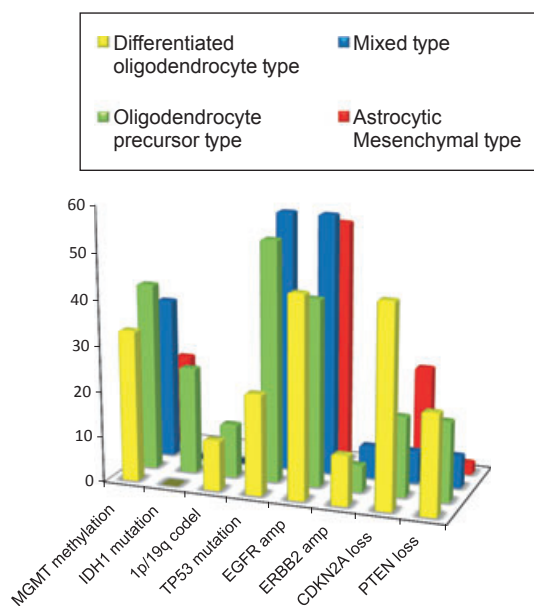


Fig. 7. Frequency and pattern of genetic and epigenetic alterations in four glioblastoma multiforme (GBM) subtypes.

expression profile has not been described elsewhere. However, the limitation of unsupervised clustering, which does not guarantee a clinically relevant classification, must be considered. Among the four clusters, the OPC and AsMes types in particular showed unique immunohistochemical patterns.

In addition, the survival patterns of the patients with GBM tumors classified into these types were significantly different. The OPC type was characterized by a favorable outcome and high positivity for Olig2, PDGFRA and IDH1-R132H on the immunohistochemical staining. The Kaplan–Meier log-rank test revealed that the OPC type was associated with a median

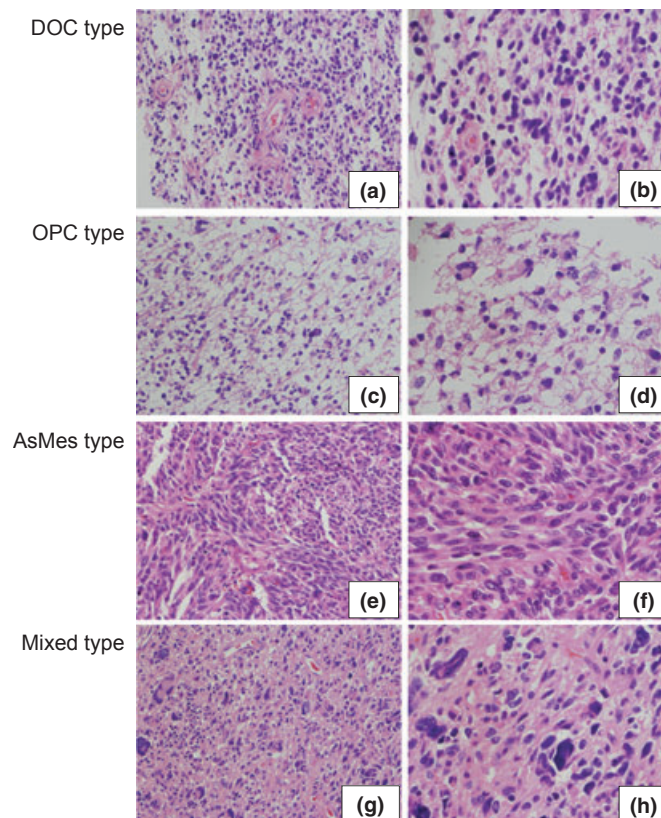


Fig. 8. Morphological findings of four types on the H&E sections. In the Differentiated Oligodendrocyte (DOC) type (original magnification: (a) $\times 20$; (b) $\times 40$), the tumor cells have small round/oval nuclei and indistinct processes. In the Oligodendrocyte Precursor (OPC) type (original magnification: (c) $\times 20$; (d) $\times 40$), there are scattered intermediate to large pleomorphic and/or multinucleated cells. In the Astrocytic Mesenchymal (AsMes) type (original magnification: (e) $\times 20$; (f) $\times 40$), spindle-shaped cytoplasmic processes are distinct and form bundles in an interlacing fashion. In the Mixed type (original magnification: (g) $\times 20$; (h) $\times 40$), in the background of small-sized to intermediate-sized spindle-shaped cells arranged in a haphazard fashion, there are several pleomorphic large cells.

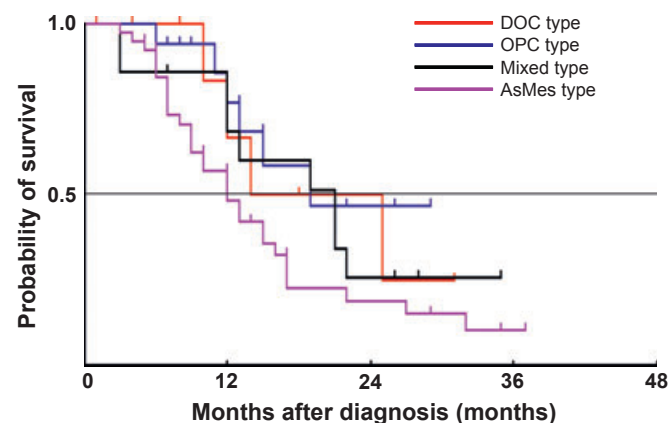


Fig. 9. Kaplan–Meier estimates of overall survival (OS) for all the glioblastoma multiforme (GBM) patients ($n = 79$) separated into four subgroups.

OS of 19.9 months (Fig. 9). This is possibly a result of the high positive score for IDH1-R132H, which is well recognized as a predictive biomarker and may influence this favorable sur-

Table 2. Median overall survival of each of the four glioblastoma multiforme subtypes

	Median overall survival (months)	95% CI
Proteomic clusters		
OPC type	19.9†	8.3–31.4
DOC type	14.8	2.6–27.0
Mixed type	21.3	7.9–34.8
AsMes type	12.8	10.0–15.7

†The median overall survival of the OPC type was significantly longer (19.9 months [95% CI, 8.3–31.4]) than that of the AsMes type (12.8 months [95% CI, 10.0–15.7]) ($P = 0.041$). AsMes, astrocytic mesenchymal; DOC, differentiated oligodendrocyte. OPC, oligodendrocyte precursor.

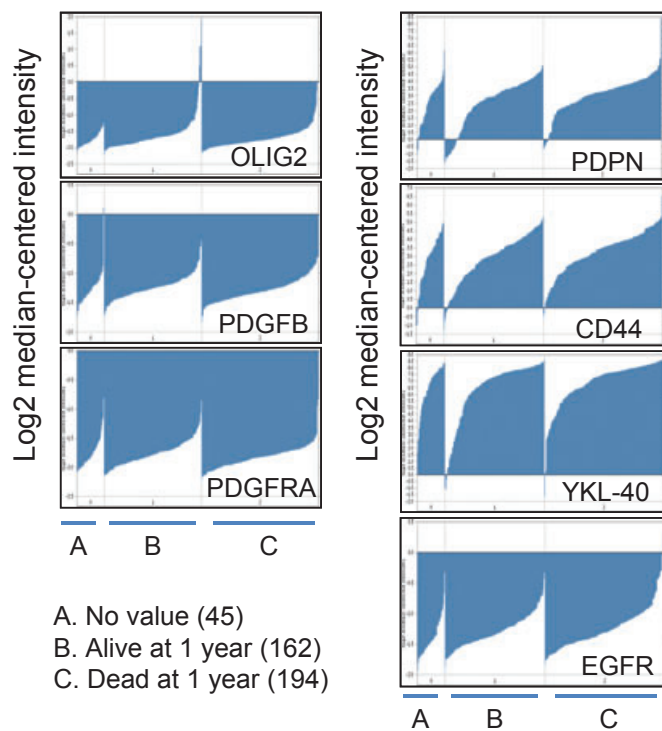


Fig. 10. Seven factors among our 16 markers that are correlated significantly with clinical outcomes from TCGA datasets. B and C show the log2 median-centered intensity of tumors of patients who were alive or dead at 1 year, respectively.

Table 3. Underexpression: dead at 1 year

Gene symbol	Reporter ID	t-test	P-value	Q-value	Fold change
OLIG2	213824_at	-2.105792	0.018113879	0.220443238	-1.0732534
PDGFB	217112_at	-2.3643584	0.009313148	0.188830637	-1.0354494
PDGFRA	211533_at	-2.8829412	0.002104464	0.141673037	-1.0440509

Table 4. Overexpression: dead at 1 year

Gene symbol	Reporter ID	t-test	P-value	Q-value	Fold change
PDPN	204879_at	3.4651806	3.04E-04	0.322990973	1.4722846
CD44	204490_s_at	2.6668687	0.004021729	0.527154075	1.296043
YKL-40	209395_at	2.2250252	0.013421925	0.672091602	1.3869164
EGFR	211551_at	1.8736842	0.030904011	0.840823061	1.0449007

vival in GBM. Oligodendrocyte precursor cells are thought to develop from neural stem cells through multiple genetic and morphological changes.⁽²⁹⁾ Oligodendrocyte precursor cells express Olig1, Olig2, Sox10, Nkx2.2⁽³⁰⁾ and PDGFRA.^(31,32) In particular, PDGFRA signaling is known to regulate the proliferation of oligodendrocyte precursor cells during neonatal development and regeneration in adulthood.⁽³³⁾

In contrast, the characteristics of the AsMes type were high positivity for PDPN and CD44 in the stroma and GFAP in tumor cells. PDPN is a mucin-like transmembrane sialoglycoprotein putatively involved in migration, invasion, metastasis and malignant progression of several tumors, such as squamous cell carcinomas, mesothelioma and testicular tumors.^(34–36) Furthermore, PDPN expression is thought to be associated with malignant progression of astrocytomas.⁽³⁷⁾ A study showed the presence of putative binding sites for NF1 within the basic transcription factor of the PDPN promoter lesion,⁽³⁸⁾ suggesting that NF1 negatively downregulates the expression of PDPN. CD44 is a major cell surface hyaluronan receptor and cancer stem cell marker that has been implicated in the progression of various cancer types.⁽³⁹⁾ Recently, CD44 was found to be upregulated in a broad range of GBM, and its elevated expression was correlated with poor prognosis.⁽⁴⁰⁾ An interesting finding is that CD44 and PDPN colocalize on cell surface protrusions in carcinoma cells, and the PDPN-CD44 interaction is important for driving directional cell migration in malignant tumors.⁽⁴¹⁾

The DOC type was clustered adjacent to the OPC type, suggesting that these clusters are closer to each other than to the other two clusters. A unique characteristic of the DOC type was that high positivity for Olig2 was observed in all the tumor sections in this cluster, whereas the positivity for the other markers was unremarkable. Genetically, the highest frequency of 1p/19q co-deletion, which refers to the combination of both 1p and 19q partial loss, and both hemizygous and homozygous deletions of the *CDKN2A* gene were observed in this class. This type is a heterogeneous group consisting of either 1p/19q co-deletion or *CDKN2A*-loss tumors. Taken together, this class may be differentiated into an oligodendroglioma-like lineage from oligodendrocyte precursor cells. The Mixed type was indeed mixed between the OPC and AsMes types. Moreover, PCA revealed that this type was a combination of the OPC and AsMes types.

Comparison with The Cancer Genome Atlas subclassification and validation of The Cancer Genome Atlas brain dataset. Mutations of the *IDH1* and *TP53* genes and high expression levels and high copy numbers of *PDGFRA* were frequently observed in the Proneural subtype advocated by Phillips and Verhaak,^(5,26) suggesting that the OPC type is similar to the Proneural type. Striking characteristics common to the OPC type and the DOC type were high Olig2 expression and low

expression levels of GFAP. However, the OPC type was characterized by higher positive scores for PDGFRA, p16, p53 and synaptophysin. The OPC type may be a mixture of Proneural and Neural subtypes.

In the Classical subtype, *EGFR* amplification and *CDKN2A* homozygous deletions were the frequent genetic alterations observed. Moreover, components of the nestin and Notch signaling pathways were highly expressed. According to our classification, overexpression of *EGFR* and the downstream effector of Notch signaling *Hes-1* were most frequently observed in the Mixed type. Deletion of *CDKN2A* and downregulation of p16 were characteristic of the DOC type, and strong nestin expression was most frequently observed in the AsMes type. The Mesenchymal subtype was characterized by high expression levels of YKL-40 and MET and high frequency of *NF1* mutation/deletion. In our dataset, the mesenchymal markers PDPN and CD44 were highly expressed in the AsMes type, which is also characterized by strong GFAP expression. The combination of higher activity of mesenchymal and astrocytic markers is suggestive of an epithelial-to-mesenchymal transition.

In the present study, the outcomes of the patients with the OPC and AsMes types were significantly different. Contrary to Verhaak's classification, the outcomes of the patients with the OPC and AsMes types, on the basis of our classification, were significantly different.

Furthermore, we could easily distinguish these two subtypes using PDGFRA, p16, p53, PDPN and CD44, as well as the routinely used proteins, GFAP, Olig2, synaptophysin and nestin. The ability to discriminate these two subtypes will contribute to the development of different therapeutic approaches for each GBM subtype.

Although there were no independent validation samples of paraffin-embedded sections of GBM, determining the associa-

tion between the expressions of these markers and the outcomes in 406 TCGA brain datasets would be of interest. Of note, Oncomine suggested that the overexpressions of PDPN and CD44 were associated with poor prognosis, and high expression levels of Olig2 and PDGFRA in tumor cells significantly improved the patient outcome. We are currently conducting a prospective randomized clinical trial, the Japan Clinical Oncology Group Study 0911, to validate the additive efficacy of interferon- β in 120 patients with newly diagnosed GBM.^(42,43) It is anticipated that his clinical trial will validate our immunohistochemical approach.

In conclusion, the data obtained by expression profiling of 79 GBM tumors based on immunohistochemical studies suggest the existence of four proteomic subgroups of GBM tumors. To the best of our knowledge, this is the first study to establish the subclassification of GBM on the basis of immunohistochemical analysis. Among the four subtypes, the patients with the OPC type showed favorable outcomes. To develop more effective and less toxic GBM treatment regimens, it is necessary to identify and correctly classify the proteomic subtypes, as well as understand the underlying oncogenic driving pathways for each type.

Acknowledgments

The authors would like to thank Mr Akiyoshi Sakai (Clinical Laboratory, Kariya Toyota General Hospital, Kariya, Japan) and Mr Hideaki Maruse, Mr Takafumi Fukui and Mr. Yosuke Furui (FALCO Biosystems, Kyoto, Japan) for wonderful technical assistance.

Disclosure Statement

Kazuya Motomura was supported by a Grant-in-Aid (B) for Scientific Research from the Ministry of Health, Labor, and Welfare, Japan.

References

- 1 Network CGAR. Comprehensive genomic characterization defines human glioblastoma genes and core pathways. *Nature* 2008; **455**: 1061–8.
- 2 Parsons DW, Jones S, Zhang X *et al*. An integrated genomic analysis of human glioblastoma multiforme. *Science* 2008; **321**: 1807–12.
- 3 Noshmeh H, Weisenberger DJ, Diefes K *et al*. Identification of a CpG island methylator phenotype that defines a distinct subgroup of glioma. *Cancer Cell* 2010; **17**: 510–22.
- 4 Kim TM, Huang W, Park R, Park PJ, Johnson MD. A developmental taxonomy of glioblastoma defined and maintained by MicroRNAs. *Cancer Res* 2011; **71**: 3387–99.
- 5 Verhaak RG, Hoadley KA, Purdom E *et al*. Integrated genomic analysis identifies clinically relevant subtypes of glioblastoma characterized by abnormalities in PDGFRA, IDH1, EGFR, and NF1. *Cancer Cell* 2010; **17**: 98–110.
- 6 Northcott PA, Korshunov A, Witt H *et al*. Medulloblastoma comprises four distinct molecular variants. *J Clin Oncol* 2011; **29**: 1408–14.
- 7 Kato Y, Jin G, Kuan CT, McLendon RE, Yan H, Bigner DD. A monoclonal antibody IMab-1 specifically recognizes IDH1R132H, the most common glioma-derived mutation. *Biochem Biophys Res Commun* 2009; **390**: 547–51.
- 8 Louis DN, Ohgaki H, Wiestler OD *et al*. The 2007 WHO classification of tumours of the central nervous system. *Acta Neuropathol* 2007; **114**: 97–109.
- 9 Kleihues P, Cavenee WK. *WHO Classification of Tumours of the Central Nervous System*. Lyon: WHO Press, 2000.
- 10 Motomura K, Natsume A, Kishida Y *et al*. Benefits of interferon-beta and temozolomide combination therapy for newly diagnosed primary glioblastoma with the unmethylated MGMT promoter: a multicenter study. *Cancer* 2011; **117**: 1721–30.
- 11 Watanabe R, Nakasu Y, Tashiro H *et al*. O6-methylguanine DNA methyltransferase expression in tumor cells predicts outcome of radiotherapy plus concomitant and adjuvant temozolomide therapy in patients with primary glioblastoma. *Brain Tumor Pathol* 2011; **28**: 127–35.
- 12 Franco-Hernandez C, Martinez-Glez V, Alonso ME *et al*. Gene dosage and mutational analyses of EGFR in oligodendrogliomas. *Int J Oncol* 2007; **30**: 209–15.
- 13 Jeuken J, Cornelissen S, Boots-Sprenger S, Gijzen S, Wesseling P. Multiplex ligation-dependent probe amplification: a diagnostic tool for simultaneous identification of different genetic markers in glial tumors. *J Mol Diagn* 2006; **8**: 433–43.
- 14 Schouten JP, McElgunn CJ, Waaijer R, Zwijnenburg D, Diepvens F, Pals G. Relative quantification of 40 nucleic acid sequences by multiplex ligation-dependent probe amplification. *Nucleic Acids Res* 2002; **30**: e57.
- 15 Martinez-Glez V, Franco-Hernandez C, Lomas J *et al*. Multiplex ligation-dependent probe amplification (MLPA) screening in meningioma. *Cancer Genet Cytogenet* 2007; **173**: 170–2.
- 16 Natsume A, Wakabayashi T, Tsujimura K *et al*. The DNA demethylating agent 5-aza-2'-deoxycytidine activates NY-ESO-1 antigenicity in orthotopic human glioma. *Int J Cancer* 2008; **122**: 2542–53.
- 17 Oi S, Natsume A, Ito M *et al*. Synergistic induction of NY-ESO-1 antigen expression by a novel histone deacetylase inhibitor, valproic acid, with 5-aza-2'-deoxycytidine in glioma cells. *J Neurooncol* 2009; **92**: 15–22.
- 18 Nobusawa S, Watanabe T, Kleihues P, Ohgaki H. IDH1 mutations as molecular signature and predictive factor of secondary glioblastomas. *Clin Cancer Res* 2009; **15**: 6002–7.
- 19 Fults D, Brockmeyer D, Tullous MW, Pedone CA, Cawthon RM. p53 mutation loss of heterozygosity on chromosomes 17 and 10 during human astrocytoma progression. *Cancer Res* 1992; **52**: 674–9.
- 20 Hartmann C, Meyer J, Balss J *et al*. Type and frequency of IDH1 and IDH2 mutations are related to astrocytic and oligodendroglial differentiation and age: a study of 1,010 diffuse gliomas. *Acta Neuropathol* 2009; **118**: 469–74.
- 21 Monti S, Tamayo P, Mesirov J, Golub T. Consensus clustering: a resampling-based method for class discovery and visualization of gene expression microarray data. *Machine Learning* 2003; **52**: 91–118.
- 22 Rousseeuw PJ. Silhouettes – A graphical aid to the interpretation and validation of cluster-analysis. *J Comput Appl Math* 1987; **20**: 53–65.
- 23 Team RDC. *A Language and Environment for Statistical Computing*. Vienna, Austria: R Foundation for Statistical Computing, 2008.
- 24 Stupp R, Mason WP, van den Bent MJ *et al*. Radiotherapy plus concomitant and adjuvant temozolomide for glioblastoma. *N Engl J Med* 2005; **352**: 987–96.
- 25 Yan H, Parsons DW, Jin G *et al*. IDH1 and IDH2 mutations in gliomas. *N Engl J Med* 2009; **360**: 765–73.

- 26 Phillips HS, Kharbanda S, Chen R *et al.* Molecular subclasses of high-grade glioma predict prognosis, delineate a pattern of disease progression, and resemble stages in neurogenesis. *Cancer Cell* 2006; **9**: 157–73.
- 27 Brennan C, Momota H, Hambarzumyan D *et al.* Glioblastoma subclasses can be defined by activity among signal transduction pathways and associated genomic alterations. *PLoS One* 2009; **4**: e7752.
- 28 Gravendeel LA, Kouwenhoven MC, Gevaert O *et al.* Intrinsic gene expression profiles of gliomas are a better predictor of survival than histology. *Cancer Res* 2009; **69**: 9065–72.
- 29 Nicolay DJ, Doucette JR, Nazarali AJ. Transcriptional control of oligodendrogenesis. *Glia* 2007; **55**: 1287–99.
- 30 Hu BY, Du ZW, Li XJ, Ayala M, Zhang SC. Human oligodendrocytes from embryonic stem cells: conserved SHH signaling networks and divergent FGF effects. *Development* 2009; **136**: 1443–52.
- 31 Levine JM, Reynolds R, Fawcett JW. The oligodendrocyte precursor cell in health and disease. *Trends Neurosci* 2001; **24**: 39–47.
- 32 Nishiyama A, Lin XH, Giese N, Heldin CH, Stallcup WB. Co-localization of NG2 proteoglycan and PDGF alpha-receptor on O2A progenitor cells in the developing rat brain. *J Neurosci Res* 1996; **43**: 299–314.
- 33 Rao RC, Boyd J, Padmanabhan R, Chenoweth JG, McKay RD. Efficient serum-free derivation of oligodendrocyte precursors from neural stem cell-enriched cultures. *Stem Cells* 2009; **27**: 116–25.
- 34 Kato Y, Kaneko M, Sata M, Fujita N, Tsuruo T, Osawa M. Enhanced expression of Aggrus (T1alpha/podoplanin), a platelet-aggregation-inducing factor in lung squamous cell carcinoma. *Tumour Biol* 2005; **26**: 195–200.
- 35 Kato Y, Sasagawa I, Kaneko M, Osawa M, Fujita N, Tsuruo T. Aggrus: a diagnostic marker that distinguishes seminoma from embryonal carcinoma in testicular germ cell tumors. *Oncogene* 2004; **23**: 8552–6.
- 36 Kato Y, Kaneko MK, Kuno A *et al.* Inhibition of tumor cell-induced platelet aggregation using a novel anti-podoplanin antibody reacting with its platelet-aggregation-stimulating domain. *Biochem Biophys Res Commun* 2006; **349**: 1301–7.
- 37 Mishima K, Kato Y, Kaneko MK, Nishikawa R, Hirose T, Matsutani M. Increased expression of podoplanin in malignant astrocytic tumors as a novel molecular marker of malignant progression. *Acta Neuropathol* 2006; **111**: 483–8.
- 38 Hantusch B, Kalt R, Krieger S, Puri C, Kerjaschki D. Sp1/Sp3 and DNA-methylation contribute to basal transcriptional activation of human podoplanin in MG63 versus Saos-2 osteoblastic cells. *BMC Mol Biol* 2007; **8**: 20.
- 39 Stamenkovic I, Yu Q. Shedding light on proteolytic cleavage of CD44: the responsible shedase and functional significance of shedding. *J Invest Dermatol* 2009; **129**: 1321–4.
- 40 Xu Y, Stamenkovic I, Yu Q. CD44 attenuates activation of the hippo signaling pathway and is a prime therapeutic target for glioblastoma. *Cancer Res* 2010; **70**: 2455–64.
- 41 Martin-Villar E, Fernandez-Munoz B, Parsons M *et al.* Podoplanin associates with CD44 to promote directional cell migration. *Mol Biol Cell* 2010; **21**: 4387–99.
- 42 Wakabayashi T, Kayama T, Nishikawa R *et al.* A multicenter phase I trial of interferon-beta and temozolomide combination therapy for high-grade gliomas (INTEGRA Study). *Jpn J Clin Oncol* 2008; **38**: 715–8.
- 43 Wakabayashi T, Kayama T, Nishikawa R *et al.* A multicenter phase I trial of combination therapy with interferon-beta and temozolomide for high-grade gliomas (INTEGRA study): the final report. *J Neurooncol* 2011; **104**: 573–7.

Supporting Information

Additional Supporting Information may be found in the online version of this article:

Table S1. Antibodies and immunostaining conditions.

Table S2. Scoring system for immunohistochemical positivity used in this study.

Table S3. Clinical characteristics of the four GBM subtypes.

Table S4. Scores of all immunohistochemical analysis and genetic/epigenetic data lists for all the analyses.

Table S5. Significant pairwise correlation coefficients derived from the Kruskal–Wallis rank test of the expressions of 16 proteins in the four GBM subgroups.

Table S6. Significant pairwise correlation coefficients derived from the Kruskal–Wallis rank test of the genetic and epigenetic alterations in the four GBM subgroups.

Please note: Wiley-Blackwell are not responsible for the content or functionality of any supporting materials supplied by the authors. Any queries (other than missing material) should be directed to the corresponding author for the article.